INSTITUTE OF PHYSICS PUBLISHING PHYSICAL BIOLOGY
Phys. Biol. **2** (2005) 111–122 doi:10.1088/1478-3975/2/2/004

# Serial rebinding of ligands to clustered receptors as exemplified by bacterial chemotaxis

**Steven S Andrews**

Physical Biosciences Division, Lawrence Berkeley National Laboratory, 1 Cyclotron Road, MS 977-152, Berkeley, CA 94720, USA

E-mail: ssandrews@lbl.gov

Received 5 May 2005
Accepted for publication 12 May 2005
Published 6 June 2005
Online at stacks.iop.org/PhysBio/2/111

**Abstract**

Serial ligation is the repeated reversible binding of a ligand to one receptor after another. It is a widespread phenomenon throughout biochemical systems, occurring anytime receptors are clustered together and ligand binding is reversible. Computer simulations are used in this work to investigate a representative example, which is the serial ligation of an extracellular aspartate molecule to the membrane-bound chemotaxis receptors of an *Escherichia coli* bacterium. It is found that the initial binding site of a ligand to a cluster of receptors is more likely to be near the edge of the cluster than near the middle, although there is no overall bias when all rebindings are considered. Serial ligation does not lead directly to signal amplification or attenuation but instead causes binding events to be correlated in both space and time: a ligand is likely to bind many times in rapid succession in a small region of the receptor cluster, but there can also be long intervals between bindings. This leads to an increased level of noise in the received signal but may allow a single ligand to be sensed above a uniform level of background noise. The focus of this paper is on the interpretation of simulation results so they can be generalized to a wide variety of other systems and to allow the identification of systems in which serial ligation is likely to be important. In the process, several characteristic times are identified, as are scaling laws for the spatial and temporal dynamics.

## Nomenclature

*Roman symbols*

| | |
|---|---|
| $D$ | diffusion coefficient |
| $d$ | average separation between receptors |
| $k_b$ | binding rate constant |
| $k_u$ | unbinding rate constant |
| $N$ | expected number of different receptors that one ligand binds to |
| $R$ | radius of receptor cluster, or of sphere for unclustered receptors |
| $t$ | time |
| $V$ | simulation volume |

*Greek symbols*

| | |
|---|---|
| $\phi$ | probability of geminate recombination |
| $\sigma_b$ | binding radius |
| $\sigma_u$ | unbinding radius |
| $\tau_{\text{gem.}}$ | characteristic time for geminate rebinding |
| $\tau_{\text{n.g.}}$ | characteristic time for non-geminate rebinding |
| $\tau_{\text{ter.}}$ | characteristic time for termination of rebinding |
| $\tau_{\text{total}}$ | typical duration of influence for one ligand |
| $\tau_u$ | characteristic time for unbinding |

## 1. Introduction

*Escherichia coli* bacteria have a cluster of chemotaxis receptors localized to one pole of the bacterium, which are used to detect attractant and repellent molecules. There is increasing evidence that the receptors are clustered, and are coupled with several intracellular proteins, to create a highly interconnected signaling module which can respond to chemoattractants over a very wide range of concentrations

  

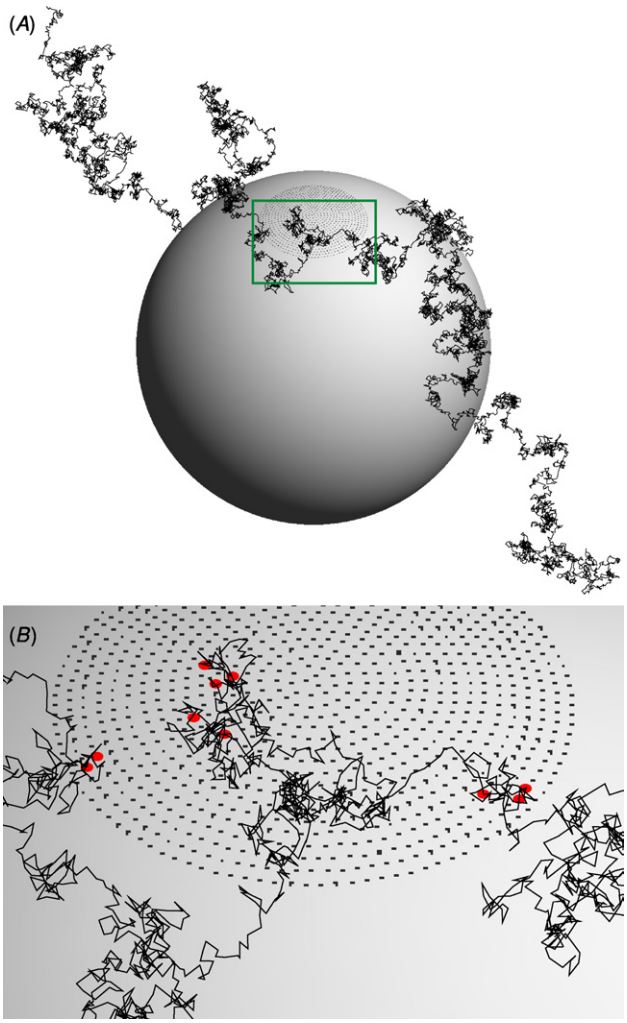


**Figure 1.** The model system with clustered receptors, shown as (*A*) the entire system and (*B*) a close-up view of the receptor cluster. The 1.5 $\mu$m diameter sphere represents an *E. coli* bacterium. At the top of the sphere, there are about 3000 receptors clustered together in a 450 nm diameter patch, although only 1000 receptors are shown in this figure for clarity. The Brownian motion trajectory of a single ligand is shown starting on the top left of the figure, binding to several receptors sequentially, and ending at the bottom right of the figure. Binding sites are shown in (*B*) with red dots.

[1]. Because ligand binding is reversible, another outcome of the receptors being clustered is that a single ligand molecule is likely to bind to several receptors sequentially (figure 1). This phenomenon, in which a molecule binds to one receptor, and then another, and another and so on, is called either *ligand rebinding* or *serial ligation*. The repeated binding of a ligand to the same receptor is called *geminate recombination* [2]. These phenomena lead to spatially and temporally correlated chemical reactions. Downstream in the signaling network, the correlated bindings may produce intermittent bursts of activity.

Correlated reactions are an important source of intracellular noise in gene expression, where the correlations arise from the sequential transcription and translation of DNA to mRNA to protein, and from sequential regulatory steps [3]. These yield short bursts of protein synthesis that can be harmful for some cellular processes, such as circadian clocks [4], or can be beneficial for providing non-genetic individuality [5]. The ultimate origin of gene expression noise is from the discreteness of molecules, because there tend to be large relative fluctuations for molecules that are produced with low copy numbers. Serial ligation is fundamentally different: it is still the case that the noise is largest when there are few molecules and that there is stochasticity that arises from the discreteness of molecules, but now additional stochasticity arises from *Brownian motion*. Little work has been done to quantify the correlations produced by serial ligation or to determine the situations in which it is likely to be biologically important. Stochasticity and reaction correlations that arise from spatial processes are ignored by nearly all simulation algorithms, including those that are called exact [6, 7].

Most prior work on serial ligation has focused on the rebinding of ligands to an infinite planar surface that is uniformly covered with a continuous density of binding sites, leading to results that are particularly useful for surface-based experiments such as surface plasmon resonance and total internal reflection microscopy [8–12]. Other work has studied geminate recombination in detail for isolated receptor–ligand pairs [13, 14] and time-averaged binding rates for reactive patches on spheres [15–17]. The application of these studies to biological systems and to biological modeling can be unclear. More specialized studies have investigated serial ligation to T-cell receptors [18, 19] and signaling in a synaptic cleft using many ligands [20, 21].

This paper explores serial ligation for a model system that is loosely based on the *E. coli* receptor cluster, focusing on the general consequences of serial ligation and the situations in which it is likely to be biologically significant. Spatial binding patterns and temporal correlations of bindings are investigated.

## 2. The model system

Most of the *E. coli* chemotactic receptors are localized to a patch at a cell pole that is about 450 nm in diameter [22, 23]. The cluster contains several types of transmembrane receptors which are probably randomly mixed [24, 25] and spaced about 7.5 nm apart from each other [26, 27]. The extracellular domains of the receptors are in a densely packed 10 nm thick region between the inner and outer cell membranes called the periplasm, where they encounter attractant and repellent molecules that diffuse in from the surrounding medium. Some of these molecules, such as serine and aspartate, diffuse rapidly into the periplasm through large channels in the outer membrane while others, such as maltose and nickel ions, encounter specific binding proteins in the periplasm and then bind to receptors in this form [28].

In the model investigated here, the ordinarily rod-shaped bacterium with hemispherical ends is simplified to a 1.5 $\mu$m diameter sphere (figure 1). Receptors are arranged in either a 450 nm diameter cluster or are evenly distributed over the whole sphere to provide an unclustered reference system; the cluster radius is denoted as $R$. Receptors are spaced evenly along 'latitude' lines, where the distance between receptors on a line is equal to the distance between lines. Because

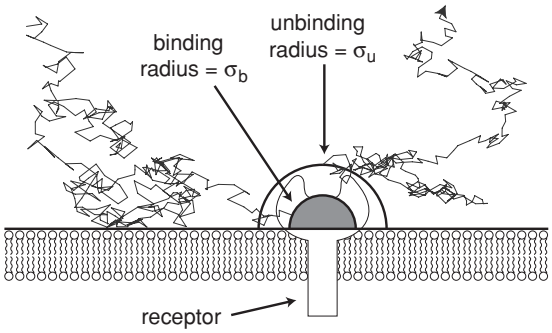


**Figure 2.** Details of ligand binding to a single receptor. The physical system includes the lipid bilayer and a transmembrane receptor. Heavier lines show its computational representation, comprising a smooth surface to represent the outside of the membrane and hemispheres to mark the binding and unbinding radii. A ligand binds to the receptor when it first crosses the spherical shell with radius $\sigma_b$. Subsequent unbinding is carried out by placing the ligand at distance $\sigma_u$ away from the membrane surface.

of discretization effects, the receptor lattice cannot be made uniform with 3000 receptors, but instead, 3192 receptors are used for the clustered case and 3029 receptors for the unclustered case. The distance between nearest neighboring receptors ($d$) is about 7.2 nm and 48.1 nm, for the respective systems. Away from receptors, the surface of the sphere is a simple impermeable surface. The cell periplasm is not included in the model because preliminary results showed that it has a minimal effect on rebinding phenomena, while simultaneously complicating the discussion and reducing the generality of results.

Only a single ligand is considered at a time, both to simplify the analysis and because rebinding is likely to be most biologically significant with low ligand concentrations. Clearly, if some receptors are already occupied, then the possible consequences of the rebinding of any individual ligand will be decreased and the number of rebindings is likely to be reduced due to competition from other ligand molecules. This ligand is treated as a point-like particle with continuously variable $x$, $y$ and $z$ coordinates, which diffuses throughout the extracellular environment by simple Brownian motion. The ligand binds to a receptor at the first moment that it diffuses to within the *binding radius* ($\sigma_b$) of the receptor's center [29, 30] (figure 2). When it is subsequently released from the receptor, it is released in the direction perpendicular to the plane of the membrane, at a distance called the *unbinding radius* ($\sigma_u$), which is larger than the binding radius. These radii are derived and justified below.

All of the receptors in this model are based on the *E. coli* Tar protein and the ligand is based on aspartate, because this receptor–ligand pair has been studied thoroughly. The diffusion coefficient of aspartate ($D$) is about $5 \times 10^{-6}\,\mathrm{cm^2\,s^{-1}}$ [15]. Receptors are treated as though they are immobile, at least on the timescale of a simulation. The binding rate constant for aspartate to Tar ($k_b$) is about $10^9\ \mathrm{M^{-1}\ s^{-1}}$ [31] and the dissociation rate ($k_u$) is about $10^3\ \mathrm{s^{-1}}$ [31, 32]. These parameters are used in all simulation results presented here. The more general conclusions that are presented below were also verified using several different sets of parameters.

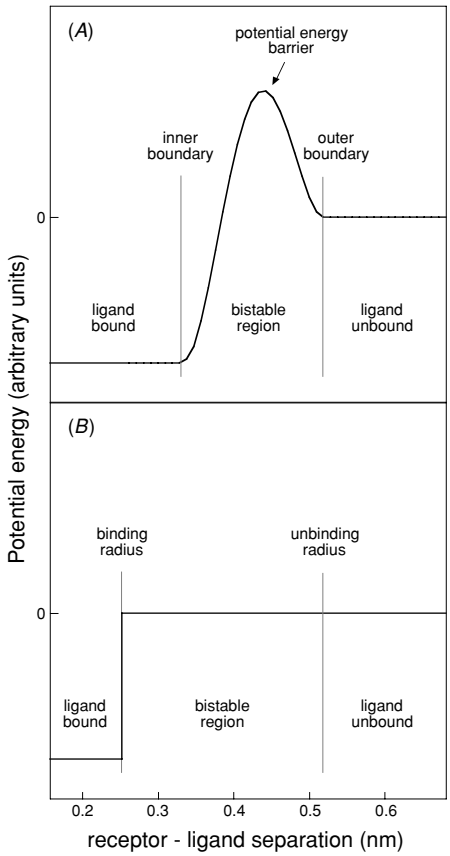


**Figure 3.** Interpretation of binding and unbinding radii. (*A*) Potential energy as a function of the distance between the receptor's active site and the center of the ligand. A ligand is considered to bind when it crosses the inner boundary and unbind when it crosses the outer boundary. (*B*) Simplified interaction region used in this paper. This is easy to simulate and analyze, while behaving nearly identically to the more accurate version. Binding and unbinding radii are shown with the values chosen in the main text.

## 3. Binding and unbinding radii, and geminate rebinding

An accurate treatment of receptor–ligand interactions would account for all the interactions that occur at short distances, such as electrostatic forces, bonding interactions and solvation effects, many of which depend on the ligand's orientation. It is conventional to simplify these to a potential energy function of a one-dimensional reaction coordinate, where this coordinate is essentially the distance between the receptor's active site and the center of the ligand (figure 3(*A*)) [33]. The steady-state binding reaction rate depends primarily on the height and position of the potential barrier, where the latter dependence arises from the higher probability of a ligand colliding with a large active site than with a small one. While it is tempting to use the peak of the potential energy curve to discriminate between a ligand-bound state and a ligand-unbound state, this is unsatisfactory: because the ligand moves by Brownian motion, this separation, or any other separation, is recrossed many times whenever the ligand gets close to it [34]. Instead, it is preferable to introduce bistability by not considering the

ligand to bind until it crosses a boundary on the inside of the potential barrier and then not considering it to unbind until it crosses a different boundary on the outside of the barrier. The outer boundary is the physical distance between the ligand and the active site of the receptor outside of which interactions are negligible, making it somewhat larger than a ligand radius. Once a ligand unbinds, it might rebind to the same receptor to yield a geminate recombination or it might diffuse away permanently. The probability of geminate recombination ($\phi$) is clearly greater if the potential barrier is low.

The source of the reaction inhibition is simplified by eliminating the potential energy barrier and using a smaller inner boundary instead, now called the binding radius (figure 3(*B*)). This radius is chosen so as not to affect the steady-state binding reaction rate, which means that the probability of geminate recombination is also unchanged (both processes depend on the probability of a ligand getting from the outer boundary to the inner boundary). While the detailed dynamics on size scales smaller than the unbinding radius are affected by this substitution, it does not matter because we are only concerned with dynamics on larger distance scales, and on time scales that are longer than the time that it takes a ligand to diffuse from $\sigma_u$ to $\sigma_b$ (quantified below). These larger scale dynamics are essentially indistinguishable between the two models [29]. This simplification is superior to the frequently used Collins and Kimball model [13, 35, 36], in which the full potential energy barrier is replaced with an infinitesimally narrow barrier, because it is conceptually and mathematically simpler and much easier to simulate, while still yielding essentially the same results on the length and time scales that are of interest [29].

If receptor–ligand interactions occurred far from a membrane, the binding radius would be [29]

$$\sigma_b = \frac{k_b}{4\pi D}(1-\phi). \tag{1}$$

However, receptors in the model are considered to be precisely at the surface of the membrane (figure 2), making only half of each receptor's binding surface accessible to a ligand. This leads to fewer receptor–ligand collisions by a factor of 2, leading to a corrected equation for membrane-bound receptors,

$$\sigma_b = \frac{k_b}{2\pi D}(1-\phi). \tag{2}$$

Because of spatial symmetry, this correction does not affect the probability of geminate recombination, which is [29]

$$\phi = \frac{\sigma_b}{\sigma_u}. \tag{3}$$

As neither $\sigma_u$ nor $\phi$ are known, they need to be estimated. Using physical arguments, it was stated that $\sigma_u$ should be somewhat larger than the ligand radius (about 0.3 nm for aspartate); also, the binding of aspartate to Tar receptors has been described as nearly *diffusion limited* [31], implying that the potential energy barrier is low and thus the probability of geminate recombination is high. Consistent with this information, as well as the experimental reaction rates and diffusion coefficient listed above, the binding radius is taken to be 0.26 nm, the unbinding radius to be 0.53 nm and the probability of geminate recombination is $\phi = 0.5$.

The binding radius is an artificial concept, but is still meaningful: its size is a measure of the intrinsic reactivity [37] of a receptor–ligand pair, analogous to a gas-phase collision cross-section [33]. Also, it provides a characteristic distance scale for receptor–ligand reactivity, which is not provided by the reaction rate constant, but which will prove to be an important parameter for assessing serial ligation.

## 4. Simulation methods

Simulations were performed with a C language computer program that uses several *Brownian dynamics* algorithms described previously [29]. Because only one ligand is considered at a time, the program could be made both fast and accurate by using adaptive time steps [38]: steps are small when a ligand is close to a receptor or the sphere surface, and large when it is far away. To yield high accuracy, the expectation displacement of the smallest diffusive steps is equal to 1% of the binding radius. Each ligand is started at a random point on a spherical shell that is just outside the surface of the sphere (plus the binding radius) because this eliminates the need to simulate the initial approach, without affecting results. A ligand escapes the system when it is 1000 sphere radii away from the sphere center, which is when its probability of ever contacting the sphere again is less than 0.1% [39] and the probability of its binding to another receptor is even lower. Collisions between the diffusing ligand and the sphere are treated with ballistic type reflections because, despite the different physical picture, this method treats Brownian motion accurately [29, 40]. Ligand unbinding is simulated using a single time step, where the length of the step is an exponentially distributed random number [41] with mean value equal to the dissociation time constant. The simulation source code can be downloaded from the World Wide Web [42].

## 5. Average properties and consistency checks

The chemical reaction considered here is simply

$$\mathrm{R} + \mathrm{L} \underset{k_u}{\overset{k_b}{\rightleftharpoons}} \mathrm{RL} \tag{4}$$

where R is a receptor and L is a ligand. As usual, the equilibrium constant is

$$K_{\mathrm{eq.}} = \frac{k_b}{k_u} = \frac{[\mathrm{RL}]}{[\mathrm{R}]\,[\mathrm{L}]}. \tag{5}$$

This can be interpreted as the equilibrium concentration ratio for many ligands, or as the time average behavior for one ligand. In either case, the system needs to be confined to a finite volume ($V$) so the ligands do not escape; also, it is independent of the physical locations of the receptors. Using the latter interpretation, equation (5) is rearranged to yield the ratio of time that a single ligand spends bound to a receptor, to the time that it is free,

$$\frac{\text{time bound}}{\text{time free}} = \frac{n_R k_b}{V k_u} \tag{6}$$

where $n_R$ is the number of receptors on the cell. Using the parameters listed above, along with a volume of 9.62 $\mu\mathrm{m}^3$, the ratio is calculated to be 0.518. In a simulation that ran for 100 s of simulated time and that used the same parameters,

the ligand bound to receptors 33 837 times for a total duration of 34.1 s while it freely diffused for the other 65.9 s, which is a ratio of 0.517. In a separate simulation with unclustered receptors, the ratio was 0.512. Both ratios are within statistical error of the theoretical result.

In a separate simulation, now without a volume constraint, the probability of geminate recombination was investigated (equation (3)). Receptors were unclustered and a ligand was started at a random receptor's unbinding radius. Of $10^5$ trials, $4.98 \times 10^4$ ligands underwent geminate recombination, which is a ratio of 0.498 and within statistical error of the theoretical answer of 0.5.

These results lend additional confidence in both the simulation program and in the logic used to derive equations (1)–(3).

## 6. Spatial dynamics

### *6.1. Initial and final binding locations*

Suppose a ligand starts so far from a cell that it is equally likely to approach the cell from any direction. To which receptor is it most likely to bind first? In the unclustered model system where receptors are uniformly distributed over the surface of a sphere, all receptors are equivalent and the initial binding site of a diffusing ligand is as likely to be at one receptor as at another. On the other hand, there is a strong bias when the receptors are clustered (figure 4(*A*)). This arises from the simple fact that the middle of the receptor cluster is surrounded by the edge of the cluster, so a randomly moving ligand is likely to strike the edge before the middle.

Two analytical solutions for the initial binding site statistics are informative. If $\sigma_b$ is very small relative to $d$, then the cluster is fairly open and the middle of the cluster is minimally 'guarded' by the edge, leading to a minimal edge effect. Alternatively, if $\sigma_b/d$ is large (it can be as large as $1/2$ without the binding radii overlapping), the receptors behave as a uniform disk that binds a ligand on the first contact. Solving the diffusion equation for this absorbing disk boundary condition [43, 44] leads to the result that the *probability density* (probability per area unit) for the initial binding position in the cluster is

$$p(r) = \frac{1}{2\pi R\sqrt{R^2 - r^2}} \tag{7}$$

where $r$ is the radius of initial binding location relative to the center of the cluster. The model situation is in between these limits since $\sigma_b/d$ is equal to 0.04. From simulation data, about 11% of the initial bindings were to a receptor on the edge of the cluster and about 82% of them were to a receptor in the outside half of the cluster (as a comparison, 6% of the receptors are on the edge and 75% are in the outside half).

Because a ligand's trajectory is simply a random walk, it is possible to consider it in the reverse direction as well, with the result that the final binding location follows the same probability density as the initial binding location. Thus, even if all receptors in a cluster were chemically identical, their relative locations would cause them to differ functionally: on average, the edge region is both the first and last part of the receptor cluster to bind a ligand.

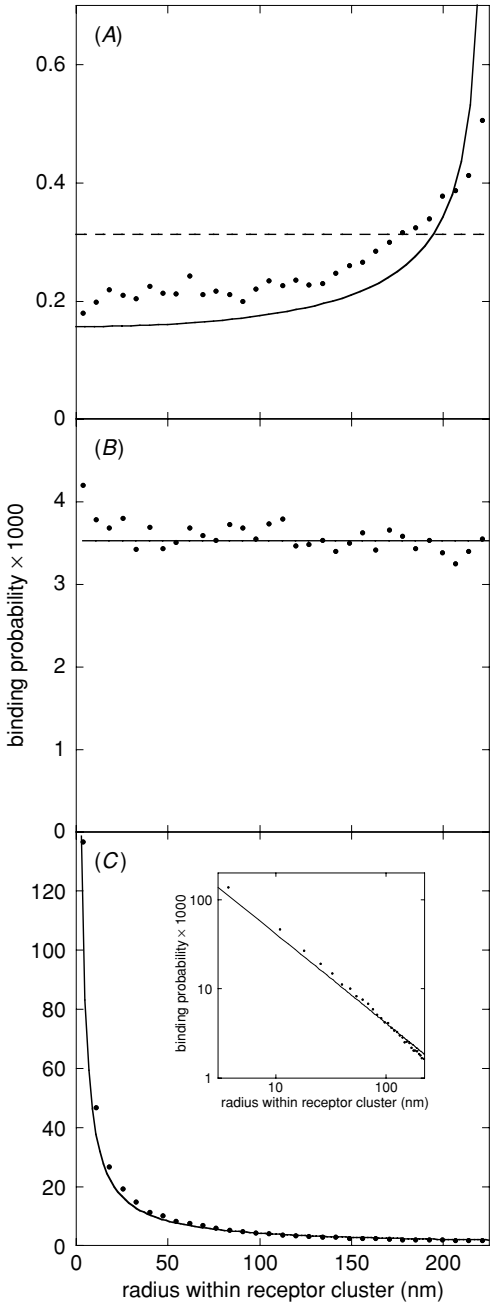


**Figure 4.** Spatial aspects of serial ligation with clustered receptors. In all cases, dots represent simulation data using $10^5$ simulated bindings and the plots show the probability that a ligand binds to a specific receptor as a function of its distance from the center of the receptor cluster. (*A*) Probabilities for the initial binding site of a ligand; the solid line is the theoretical result from equation (7) for the limit of a dense receptor cluster and the dashed line is the theoretical result for a sparse receptor cluster. Integrals under all curves are 1 (including a factor of $2\pi r$ to account for the circular cluster). (*B*) Probabilities for every binding site of a ligand; the line is the theoretical result that there is no positional bias, scaled to have the same integrated area as the simulation result (average of 11 total bindings per ligand). (*C*) Spatial correlation of bindings, shown as probabilities of all binding events using a ligand started at the center of the receptor cluster; the line is proportional to $r^{-1}$, scaled to have the same integrated area as the simulation result. The inset is identical to panel *C* but shown with log–log axes.

### 6.2. Locations of all bindings

Is there still a statistical bias towards the edge of a cluster when every binding site is considered, rather than just the initial one? Again, there is clearly no bias for unclustered receptors because they are all equivalent. Using simulations, it is also found that there is no statistically significant bias for clustered receptors (figure 4(*B*)). The explanation is that binding to and unbinding from a receptor occurs in nearly the same place, so receptors have essentially no effect on the spatial trajectory of the diffusing ligand, seen qualitatively in figure 1. Binding to a receptor only delays the ligand, leaving the spatial trajectory as a simple random walk near an impermeable surface.

An implication is that a cluster of receptors (that bind reversibly) does not affect the probability of finding an unbound ligand nearby. The same result, but for many ligands, is that receptors do not affect the local concentration of unbound ligands. Statistical mechanics provides an alternate explanation for this result: the probability that a ligand is in a particular region is proportional to $\exp(-\beta E)$, where $\beta$ is the Boltzmann factor and $E$ is the potential energy [33]; outside of the receptors' binding radii, the potential energy is everywhere 0, so the unbound ligand concentration is unaffected by the presence of receptors. A second implication is that a ligand is equally likely to bind to a receptor on the edge of a cluster, in the middle of a cluster or that is relatively isolated. In this respect, all receptors in a cluster behave equivalently. Finally, on average, a ligand spends the same total amount of time bound to receptors if the receptors are clustered as if they are unclustered, a result that was already quantified in equation (6). In biology, this means that the mere clustering of receptors, without allosteric interactions, can neither amplify nor attenuate a signal that is transmitted by diffusing molecules.

### 6.3. Total number of bindings

Perhaps the best way to quantify the extent of serial ligation is to find the total number of receptors to which a ligand binds, on average. This is found with the integral of the simulation data in figure 4(*B*), including a factor of $2\pi r$ to account for the circular receptor cluster, which yields the result that ligands that bind at least once end up binding an average of about 11 total times before diffusing away permanently. Half of these are geminate rebindings because of our choice of $\phi$. Removing this contribution, each ligand that binds once, binds to an average of about six different receptors over the course of its time spent in the vicinity of the cell. In contrast, it was found that ligands that bound to unclustered receptors only bound an average of three times, of which 1.5 were to different receptors. Thus, when receptors are clustered, there is an increased probability that ligands will bind multiple times; in this case, the expected number of bindings is about four times larger. Reconciling this with the prior result that receptor clustering does not affect the total number of bindings, on average, implies that four times more ligands are detected with unclustered receptors. In other words, clustered receptors lead to fewer ligands being detected and proportionately more bindings for those that are detected.

A quick calculation yields an estimate for the average total number of receptors to which a ligand binds. Starting at the center receptor and not counting geminate rebindings, the probability that a ligand ever binds to a specific nearest neighbor receptor is about $\sigma_b/d$. Considering receptors arrayed around the center one in rings that are spaced $d$ units apart, the probability of binding to a receptor on the $j$th ring is about $\sigma_b/(jd)$, and this ring has about $2\pi j$ receptors. For a radius $R$ cluster, there are about $R/d$ rings of receptors. The expectation number of different receptors that a ligand binds to ($N$) is 1 for the first binding, plus the sum of the probabilities of binding to other receptors:

$$N \approx 1 + \sum_{j=1}^{j_{\max}} 2\pi j \frac{\sigma_b}{jd} \approx 1 + \frac{2\pi R\sigma_b}{d^2}. \tag{8}$$

If a ligand binds to receptor 'A', then receptor 'B' and then 'A' again, the bindings are treated here as three separate receptors, rather than as a geminate recombination. Because the initial binding is unlikely to be at the center of the cluster, this calculation overestimates the extent of serial ligation but still provides a useful estimate. Inserting the parameters used in the simulation yields about 8 and 1.5 different receptors for the clustered and unclustered cases, respectively (for the latter, the sphere radius is used for $R$). These are close to the simulation results of 6 and 1.5; calculated values are also in reasonable agreement with simulation results that use other values of $\sigma_b$.

Thus, the extent of serial ligation can be quantified as the expectation number of different receptors to which a ligand binds, assuming it binds at all. It depends on two unitless parameters: $\sigma_b/d$, which is the probability that a ligand hops from a receptor to its neighbor, and $R/d$, which is a measure of the size of the receptor cluster.

### 6.4. Spatial correlation

Given that a ligand binds to a specific receptor, where is it likely to bind in the future? Clearly, at each rebinding, it is more likely to bind to a receptor that is nearby than to one that is far away. The simulation result shown in figure 4(*C*) was created by starting many ligands, sequentially, at the center of the receptor cluster and recording the locations of subsequent bindings. These data have a profile that is slightly steeper than a curve proportional to $r^{-1}$, where $r$ is the distance from the initial binding site. In a control simulation that modeled a cluster of receptors on a flat surface, the data exactly matched a slope of $r^{-1}$, to within statistical error, showing that the additional slope in figure 3(*C*) arises from the spherical surface of the modeled cell.

The $r^{-1}$ power law can be understood by contrasting the scaling properties of ballistic motion and Brownian motion. In unrestricted three-dimensional space, consider a set of objects that start at the origin, and that move away with a constant velocity. If they produce a fixed 'mass' of trajectory behind them during each time unit, the total mass in each spherical shell about the origin is equal and, because the volume of a spherical shell is proportional to $r^2$, the mass density falls off as $r^{-2}$. In contrast, if they move by Brownian motion, like the ligands considered here, the objects move away from

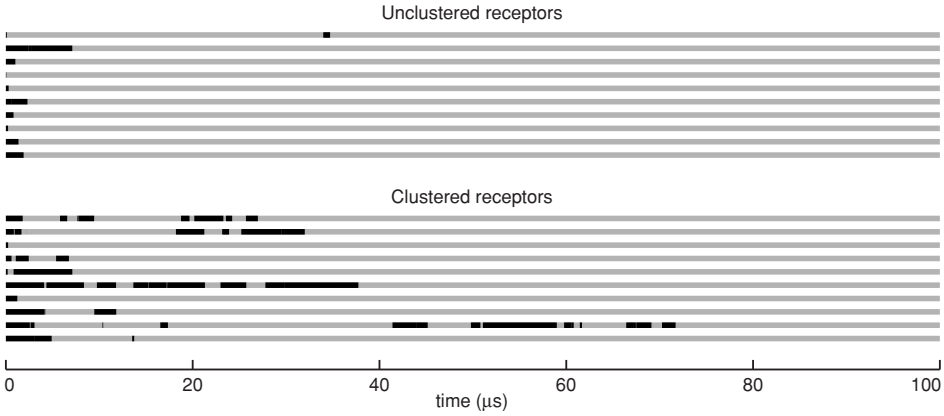


**Figure 5.** Ligand binding as a function of time for unclustered and clustered receptors to represent the signal that is detected by the cell. Each horizontal line represents a separate trial with time 0 defined as the moment that the ligand first binds to a receptor. Black bars represent times when the ligand is bound and gray gaps represent times when it is freely diffusing. To allow both the bound and unbound times to be seen on the same figure, the dissociation time constant was reduced from 1000 $\mu$s to 1 $\mu$s; despite this, most geminate rebindings occurred too quickly to be resolved here.

the origin at a rate proportional to $t^{1/2}$ rather than $t$ [45] so the mass density falls off as the square root of the previous value—now, it falls off as $r^{-1}$. This is unaffected by the presence of an impermeable planar membrane that includes the origin, due to symmetry. Thus, a receptor at distance $r$ from the origin (whether it is on the membrane or not) has a probability proportional to $r^{-1}$ of having some of the Brownian motion trajectory within its binding radius.

Restating this result for the biochemical situation, the average density of ligand bindings with receptors on a planar membrane will decrease away from the initial binding site as $r^{-1}$.

### 6.5. Domain of influence

Is there a characteristic length scale such that one can say with reasonable confidence that most bindings are within that distance of the initial binding site? For a ligand that starts at the center of the receptor cluster, the mean distance between the initial binding site and subsequent binding sites is

$$\langle r \rangle = \int_0^R 2\pi r \rho(r)\, \mathrm{d}r. \tag{9}$$

The factor of $2\pi r$ accounts for the increasing circumference at larger radii and $\rho(r)$ is the density of rebindings. It was just shown that this density is proportional to $r^{-1}$ (the relatively small effect of the curved cell surface is ignored) so the integrand is a constant and the solution is proportional to $R$. Although the upper limit of the integral is more complicated for ligands that start elsewhere, the result is still proportional to $R$. Rebindings are not localized just to the region of the first binding but are spread over the entire receptor cluster.

Alternatively, the domain of influence of a ligand could be defined as the median radius of binding, which is the radius for which half of the bindings are inside and half are outside. Again, this is found to be proportional to $R$. Thus, there is no characteristic length scale for rebinding: while most rebindings occur close together, enough are far apart that the spatial domain is limited only by the size of the receptor cluster. The domain of influence of a ligand is the entire receptor cluster.

## 7. Temporal dynamics

### 7.1. Qualitative results

In the two state model of receptor activation, a receptor is 'on' if a ligand is bound to it or 'off' when no ligand is bound [46]. Suppose the bacterial chemotaxis biochemistry depends only on the cumulative signal, which is defined as the sum of the states of all receptors. Examples of this signal are shown in figure 5 using a single ligand, where a black bar indicates that the ligand is bound and a gray interval indicates that it is freely diffusing. For presentation purposes in just figure 5, $k_u$ was increased from $10^3$ s$^{-1}$ to $10^6$ s$^{-1}$ to make the black bars a factor of 1000 shorter than they should be. In reality, an aspartate molecule spends a relatively long time bound to several Tar receptors, separated by rapid hops from one to the next.

It is seen that receptor clustering influences the number of bindings for a ligand and their relative timings. In the unclustered case, most ligands only bind once. With clustered receptors, ligands are likely to rebind quickly after each unbinding, leading to short gaps in a series of bindings. At other times, these ligands are relatively far from all receptors, leading to long gaps.

### 7.2. Distributions of bound and unbound time intervals

Figure 5 is interpreted by investigating the distributions of the lengths of the black bars and gray intervals. For the former distribution, unbinding follows first-order kinetics so the probability that the ligand unbinds during a short time interval is high initially and decreases exponentially. The time constant of unbinding is the inverse of the dissociation rate constant:

$$\tau_u = k_u^{-1}. \tag{10}$$

From the properties of an exponential, the average amount of time that a ligand spends bound to one receptor is $\tau_u$ and it is

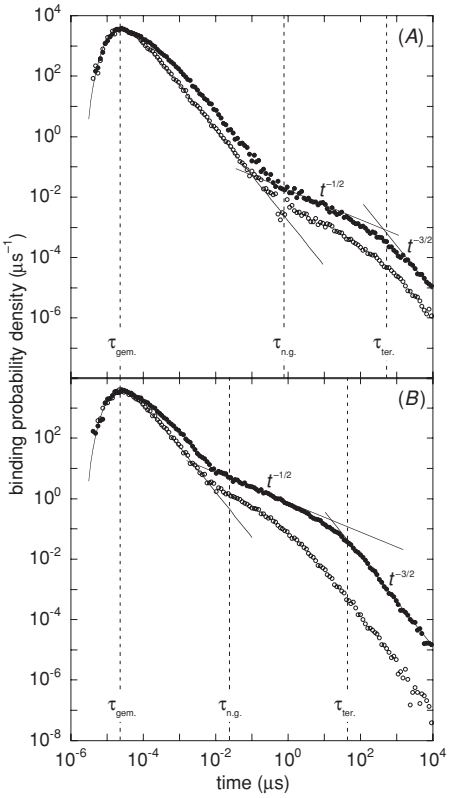


**Figure 6.** Temporal correlations arising from serial ligation. A ligand is released from the first receptor to which it bound at time 0 and then may rebind to the same or a different receptor at a later time. Shown is the probability density for this rebinding as a function of time for (*A*) unclustered and (*B*) clustered receptors, along with the relevant characteristic times that are discussed in the text. Open circles represent simulation data for the first rebinding and filled circles are simulation data for all rebindings. The solid lines shown in the early, intermediate and late portions of each panel are the theoretical probability density for geminate rebinding, a line with a time dependence of $t^{-1/2}$ and a line with time dependence proportional to $t^{-3/2}$, respectively. As the solid circles show the probability density of a rebinding occurring as a function of time, the integral under them is the expectation number of rebindings, which are about 2 and 10 for the unclustered and clustered cases, respectively.

rare for a single binding event to last more than several times $\tau_u$. A disproportionate number of black bars in figure 5 appear to be much longer than the 1 $\mu$s value of $\tau_u$ that was used to generate the figure simply because most geminate rebinding intervals are too brief to be resolved by the printer.

The intervals between bindings are more complicated because of the fractal nature of the ligand's trajectory and because there are several possible outcomes: a geminate rebinding, a non-geminate rebinding or the ligand permanently diffusing away. Also, the statistics of the intervals are slightly different for ligands that start at the edge of the receptor cluster from those that start in the middle. The distribution of intervals between bindings is shown in figure 6.

Upon release from a receptor at time 0, a ligand is distance $\sigma_u$ from the geminate receptor. It cannot rebind at this moment, although it is likely to rebind soon afterwards because the geminate receptor is only $\sigma_u - \sigma_b$ distance away, which explains the initial peaks in both panels of figure 6. This portion of the data agrees with analytical results derived in the appendix (and provides an additional consistency check between simulation and theory), where it is shown that geminate rebinding is most probable at the characteristic time

$$\tau_{\text{gem.}} = \frac{(\sigma_u - \sigma_b)^2}{6D}. \tag{11}$$

With the usual parameters, $\tau_{\text{gem.}} = 0.02$ ns for both the clustered and unclustered models. This is meaningful for the idealized system but not physically because the model is highly simplified at these small size scales. Nevertheless, the qualitative behavior is correct: the rebinding probability is very high just after unbinding and decreases for long times with a time dependence proportional to $t^{-3/2}$.

After the initial peak, the rebinding probability decreases rapidly until the ligand has had a chance to diffuse to the nearest neighboring receptors. Using the same analytical result from the appendix, non-geminate rebinding is most probable at the characteristic time

$$\tau_{\text{n.g.}} = \frac{d^2}{6D}. \tag{12}$$

These times are $\tau_{\text{n.g.}} = 0.02$ $\mu$s and 0.8 $\mu$s, for the clustered and unclustered models, respectively. They describe how long it takes a ligand to hop from receptor to receptor for a typical rebinding. After $\tau_{\text{n.g.}}$, a ligand is typically far enough from the geminate receptor that there is no longer a heightened probability of binding there, but it also has not diffused far enough for the edge of the receptor cluster or the sphere curvature to be dominant influences. During this period, the ligand's 'view' is of a very large array of receptors spread over a nearly planar surface, a situation that has been investigated previously [9–11, 47]. Here, the probability density of binding decreases proportionally to $t^{-1/2}$ because it is the product of: the probability that the ligand strikes the cell surface, called a *zero-crossing*, and the probability that there is a receptor at that site. The latter factor is a simple constant and the former is proportional to $t^{-1/2}$ using the theory of Brownian motion [45].

At even longer times, rebinding is terminated by the diffusion of the ligand away from the receptor cluster, or from the cell. The characteristic termination time is the average time a ligand takes to diffuse a distance equal to the radius of the receptor region,

$$\tau_{\text{ter.}} = \frac{R^2}{2D}. \tag{13}$$

For the clustered and unclustered models, $\tau_{\text{ter.}}$ is about 51 $\mu$s and 560 $\mu$s, respectively; in the latter case, $R$ is the sphere radius, as usual. Finally, the slope of the binding probability returns to $t^{-3/2}$, which can again be understood by considering the ligand's 'view'. After $\tau_{\text{ter.}}$, the ligand is typically far from the cell, so all the receptors together can be approximated as a small absorbing patch that is far away, in a situation that is analogous to the relationship between the ligand and the geminate receptor during the interval between $\tau_{\text{gem.}}$ and $\tau_{\text{n.g.}}$. This $t^{-3/2}$ dependence continues indefinitely after $\tau_{\text{ter.}}$.

The characteristic times are plainly evident in figure 6 and separate several temporal regions: before any rebinding, primarily geminate rebinding, serial ligation on the whole receptor cluster and rebinding is mostly complete. Because the filled circles represent the probability density of a ligand rebinding as a function of time, the integral under the data is the expected total number of rebindings. In agreement with the values presented above, these integrals, plus 1 for the initial binding, are about 11 and 3 for the clustered and unclustered models, respectively.

### *7.3. Duration of influence of one ligand*

From the time that a ligand first binds to a receptor, for how long does it stay around to exert an influence? This duration is simply the time that it spends bound to receptors plus the intervals between bindings, which is

$$\tau_{\text{total}} = \frac{N}{\phi}\tau_u + \tau_{\text{ter.}}. \tag{14}$$

With clustered receptors, a ligand spends about 11 ms in a bound state and about 51 $\mu$s diffusing in the vicinity of the cluster, showing that the vast majority of time is spent with the ligand bound. For unclustered receptors, the results are about 3 ms with the ligand bound and 0.6 ms with it diffusing.

## 8. Serial ligation of intracellular proteins

On the inside of the *E. coli* plasma membrane, the array of chemotaxis receptors forms a relatively stable complex with the downstream signaling proteins CheA and CheW. There are also more transitory engagements with freely diffusing proteins, such as the methylating and demethylating enzymes CheR and CheB, which bind to individual receptors and then detach after their catalytic action is complete. Is it possible that these cytoplasmic proteins could undergo serial ligation in an analogous fashion to that just described for aspartate on the outside of the cell? This is addressed using CheR to lend a context to work on CheR binding patterns [48] and to illustrate another use of the parameters derived above.

The number of receptors and the size of the receptor cluster is the same as before, but other parameters are quite different. Rates of protein–protein association are likely to be slower than the rate constant for aspartate binding by about three orders of magnitude, with typical rates around $10^6$ $\text{M}^{-1}$ $\text{s}^{-1}$ [49, 50]. Also, diffusion coefficients of intracellular proteins are about 200 times slower, at around $2.5 \times 10^{-8}$ $\text{cm}^2$ $\text{s}^{-1}$ [51]. Experimental results do not help with choosing either the unbinding radius or the probability of geminate recombination, so, as a first guess, $\phi$ is set to 0.5, as before. This implies that $\sigma_b$ is 0.027 nm and $\sigma_u$ is 0.053 nm. The latter parameter is ill-defined for protein–protein interactions because of the strict orientational restrictions for binding [50], but it nevertheless would be expected to be larger than the length over which there are strong chemical interactions (figure 3). In contrast, this calculated value is less than half the length of a chemical bond, making it unlikely that $\phi$ is as high as 0.5. Instead, $\sigma_u$ is chosen to be 0.53 nm to make it the same as it was for the previous discussion, and which is physically reasonable, leading to values for $\sigma_b$ of 0.05 nm and $\phi$ of 0.09. Using these parameters, the ratio $\sigma_b/d$ is 0.007, which is only a one-fifth of what it was before, indicating that there will be much less serial ligation.

The enhanced likelihood of a ligand (CheR) initially binding to the edge of the cluster rather than the middle is significantly reduced here, because of this lower value of $\sigma_b/d$, and because the system geometry is now the inside of the cell membrane. Clearly, the edge only 'guards' the middle when ligands approach from oblique angles, which is made less likely due to the concave membrane curvature. As before, CheR is equally likely to bind to any receptor when all bindings are considered.

If CheR molecules were not confined to the cytoplasm, each CheR would bind to an average of about 2.3 different receptors, using equation (8), showing that the extent of serial ligation would be minimal. However, CheR proteins are indeed confined within the cell and consequently will return an essentially infinite number of times to the receptor cluster, limited only by the protein lifetime. Since a CheR is likely to diffuse a long way between binding events, the position of each binding site is largely independent of previous binding locations.

Meaningful characteristic times for CheR bindings are the unbinding time, $\tau_u$, which is 0.1 s (based on the binding rate and the association constant of 0.09 $\mu\text{M}^{-1}$ [52]), the non-geminate rebinding time, $\tau_{\text{n.g.}}$, of about 4 $\mu$s and the termination time, $\tau_{\text{ter.}}$, of about 10 ms. Comparing $\tau_u$ with $\tau_{\text{n.g.}}$ shows that, again, binding durations last very much longer than the rapid hops that a ligand makes from one receptor to another. The termination time indicates how long a CheR spends diffusing near the receptor cluster during an average encounter.

Thus, bindings of CheR to the inside of the receptor cluster are temporally and spatially correlated due to serial ligation, although not to a great extent and to a lesser degree than for extracellular bindings of aspartate. The large differences between the rates of aspartate–Tar interactions and CheR–Tar interactions imply that it is very unlikely for there to be feedback between the behaviors of specific aspartate molecules and specific CheR proteins.

## 9. Discussion

How does serial ligation affect a transmitted signal? From very general arguments, it was shown that receptor clustering does not lead to a higher overall level of ligand binding. Instead, some aspartate molecules are detected an average of about 11 times each, while others are completely ignored. In signal processing terms, serial ligation does not amplify a signal, but increases its contrast. This behavior makes the signal received from the receptor cluster relatively noisy, which would seem to be undesirable from an engineering standpoint, but may have a biological benefit.

It has been observed in other signaling systems that the actual duration of binding can have important effects [53]. For example, ligands with a high affinity often produce larger effects than those with low affinity even when the two are

present at the same net receptor occupancy [54]. In this case, a prolonged signal generated by the rebinding of a ligand at a cluster of receptors might generate a signal large enough to switch the state of a flagellar motor [55], allowing a single ligand to be detected over stochastic noise in the signaling system.

While serial ligation undoubtedly occurs for bacterial chemotaxis, further calculations show that it is unlikely to play a significant role. There is negligible receptor sensitivity to aspartate concentrations that are below $3 \times 10^{-8}$ M [56]. This corresponds to 3% of the receptors being occupied by ligands, using the experimental dissociation constant of about $10^{-6}$ M [31], implying that about 90 different receptors are bound to aspartate at any time (using 3000 Tar receptors). This number is sufficiently large that correlations between binding times that arise from serial ligation will be minimal. Secondly, serial ligation effects are likely to be overwhelmed by the large allosteric effects that are enabled by receptor clustering [57, 1]. Nevertheless, in small regions of the receptor cluster, serial ligation may act in concert with allostery to yield noticeable effects; if so, this would most likely produce an evolutionary selection pressure.

Several experiments can be imagined that could investigate serial ligation for a system analogous to the one presented here. A conceptually simple one is a FRET measurement (fluorescence resonance energy transfer) with green fluorophore tagged chemotaxis receptors and red fluorophore tagged aspartate molecules. If the receptors were excited with blue light, the energy would be absorbed and then transferred to any bound ligands, which would emit in the red. As red emission would indicate a bound ligand, the time correlation function for red emission should be similar to the prediction shown in figure 6.

## 10. Conclusions and outlook

The dynamics of serial ligation were explored using a simple model system that is based on the binding of extracellular aspartate to the *E. coli* chemotaxis receptor cluster, which is likely to be representative of a wide variety of systems. It was found that receptor clustering, which promotes serial ligation, does not affect overall averages: a receptor is equally likely to bind a ligand if it is in a cluster or not, receptor clustering cannot lead directly to signal amplification or attenuation and clustering does not affect the concentration of free ligands in solution. Instead, serial ligation leads to binding events that are correlated in both time and space. Because of it, ligand bindings do not occur randomly, but an initial binding is likely to lead to a rapid succession of rebindings in the same region of the receptor cluster. The spatial correlation is described with a power law that is nearly proportional to $r^{-1}$ (the minor deviation arises from the curved cell surface), which is a sufficiently broad distribution that the spatial extent of rebinding is limited only by the size of the receptor cluster. Temporal correlations are more complex, with separate characteristic times for geminate rebinding, non-geminate rebinding and the termination of rebinding. Between these characteristic times, the probability of ligand rebinding is described well with power laws, with the probability decreasing as either $t^{-1/2}$ or $t^{-3/2}$, depending on the time period. As with the spatial correlation, the total time over which a ligand is likely to be detected is limited only by the size of the receptor cluster. Serial ligation increases in importance as the ratio of the binding radius to the separation between receptors increases, and as the size of the receptor cluster increases.

Several biological benefits have been studied for receptor clustering, such as allosteric interactions between receptors [1, 57], the enabling of molecular brachiation [48] and the reduction of cross-talk between different cell functions. All of these studies have ignored the effects of serial ligation, despite the fact that it is certain to occur in any biochemical system that includes reversible ligand binding. In many cases, including the chemotaxis example chosen, serial ligation is likely to play a minor role in the biochemical signal processing, although there are also situations where it could be important. If the noise in a signaling system is dominated by the statistics of receptor–ligand interactions, then serial ligation will lead to more noise in the system. On the other hand, if the dominant noise source is downstream of the receptor cluster, then the multiple bindings inherent to serial ligation can allow single ligands to be detected above the background level of noise.

In this work, serial ligation was simulated using a full three-dimensional model of the system which was computationally efficient because it treated only a single ligand at a time. However, this is not generally applicable so a challenge for theorists is to include the spatial and temporal correlations that arise from serial ligation in stochastic analyses of chemical networks, as well as in stochastic simulation algorithms. In their absence, even the so-called exact treatments are significantly in error.

This study on serial ligation is but one aspect of a growing awareness of stochastic effects in biochemistry. It is true that, on average, biology and chemistry behave according to analytically calculable averages, found from continuous chemical concentrations, reaction rate constants, dissociation constants and so on. However, specific systems at specific times are almost never average: a receptor is either active or inactive, a molecule is at one location and is not somewhere else and a membrane collision either did or did not happen. Biology evolves and operates in this real world of stochastic phenomena, making their understanding essential to an understanding of biology. These phenomena also introduce new challenges for scientists, requiring experimental methods that are not only more sensitive but that can also identify correlated events and computer programs that can efficiently handle the additional complexity.

## Acknowledgments

This work was initiated in Dennis Bray's laboratory and completed in Adam Arkin's laboratory; both advisors provided many helpful comments. Funding was provided by NIGMS grant GM64713, the Genomes to Life project of the US Department of Energy, and by an NSF postdoctoral fellowship in biological informatics.

## Appendix. Probability density for geminate rebinding

An analytic solution cannot be found for the complete temporal dynamics of serial ligation that are shown in figure 6. Instead, an exact solution for the geminate portion is calculated here, which also yields the characteristic times for geminate and non-geminate rebinding and the scaling laws for the temporal dynamics. It is found by: (i) deriving the probability density for irreversible binding to an infinite plane, and (ii) converting the result to the desired spherical system. It can also be derived from equations presented in [58].

For the planar problem, there is an infinite absorbing plane perpendicular to the $x$-axis at position $x = 0$. A single ligand, with diffusion coefficient $D$, is located on the $x$-axis at position $x = \sigma_u$, with the time started at $t = 0$. What is the probability density of the ligand's binding to the plane as a function of time? The result will be given as $b_{\text{pl.}}(t)$, where the subscript reflects the planar system. As there are no boundaries to the ligand's diffusion in the $y$ or $z$ directions, these components of the ligand's position do not influence binding to the plane and can be ignored. The spatial probability density of the ligand along the $x$ direction is denoted by $\rho_{\text{pl.}}(x, t)$, which follows the boundary conditions and diffusion equation:

$$\rho_{\text{pl.}}(x, 0) = \delta(x - \sigma_u) \tag{A1}$$

$$\rho_{\text{pl.}}(0, t) = 0 \tag{A2}$$

$$\frac{\partial}{\partial t}\rho_{\text{pl.}}(x, t) = D\frac{\partial^2}{\partial x^2}\rho_{\text{pl.}}(x, t). \tag{A3}$$

Equation (A1) expresses the known starting position of the ligand using a Dirac delta function ($\delta(x)$ equals infinity at $x = 0$ and 0 elsewhere, and has unit area) and equation (A2) expresses the fact that the plane absorbs any ligand that contacts it. The probability density $\rho_{\text{pl.}}(x, t)$ is undefined for negative $x$ values because the ligand starts with a positive $x$ value and cannot cross $x = 0$. This presents an opportunity for addressing the second boundary condition by changing the problem definition slightly to use the method of images [43, 58]: the absorbing plane is removed, $\rho_{\text{pl.}}(x, t)$ is now defined for negative $x$ values although it is not required to be physically meaningful there and a negative delta function is added to $\rho_{\text{pl.}}(x,0)$ at the mirror image of the positive delta function:

$$\rho_{\text{pl.}}(x, 0) = \delta(x - \sigma_u) - \delta(x + \sigma_u). \tag{A4}$$

This new initial condition still satisfies the first boundary condition given above for all physically meaningful $x$ values. The symmetry of the initial condition and the lack of directional bias during diffusion implies that $\rho_{\text{pl.}}(0, t) = 0$ at all times, meaning that the second boundary condition is satisfied as well, without requiring it as a separate constraint. The solution is now trivial: each delta function diffuses over time to become a Gaussian [39]:

$$\rho_{\text{pl.}}(x, t) = G_s(x - \sigma_u) - G_s(x + \sigma_u) \tag{A5}$$

$$G_s(x) \equiv \frac{1}{s\sqrt{2\pi}}\mathrm{e}^{-x^2/2s^2} \tag{A6}$$

$$s \equiv \sqrt{2Dt}. \tag{A7}$$

The probability density that a ligand binds to the absorbing plane at some time is given by the flux of $\rho_{\text{pl.}}(x, t)$ into the plane:

$$b_{\text{pl.}}(t) = D\frac{\partial}{\partial x}\rho_{\text{pl.}}(x, t)\bigg|_{x=0} = \frac{\sigma_u}{t}G_s(\sigma_u). \tag{A8}$$

This result is converted for the case of a spherical absorber. Now, there is an absorbing sphere centered at the origin with radius $\sigma_b$ and a ligand on the $x$-axis at $x = \sigma_u$ at time $t = 0$. Motion tangential to the sphere surface does not affect the solution, so the problem is made rotationally symmetric by changing the initial probability density for the ligand to a uniform spherical shell, still at radius $\sigma_u$. Using $r$ as the distance from the origin and $\rho(r, t)$ as the spatial probability density of the ligand, the boundary conditions are

$$\rho(r, 0) = \frac{1}{4\pi\sigma_u^2}\delta(r - \sigma_u) \tag{A9}$$

$$\rho(\sigma_b, t) = 0. \tag{A10}$$

Because the problem is rotationally symmetric, the diffusion equation is [43]

$$\frac{\partial}{\partial t}[r\rho(r, t)] = D\frac{\partial^2}{\partial r^2}[r\rho(r, t)]. \tag{A11}$$

Using the substitution $\rho_{\text{pl.}}(r, t) = r\rho(r, t)$, this is identical to equation (A3), allowing us to use the solution in equation (A4), along with the new boundary conditions, to yield

$$r\rho(r, t) = \frac{1}{4\pi\sigma_u^2}[G_s(r - \sigma_u) - G_s(r - 2\sigma_b + \sigma_u)]. \tag{A12}$$

The probability density flux into the sphere yields the desired result:

$$b(t) = 4\pi\sigma_b^2 D\frac{\partial\rho(r, t)}{\partial r}\bigg|_{r=\sigma_b} = \frac{\sigma_b(\sigma_u - \sigma_b)}{\sigma_u t}G_s(\sigma_u - \sigma_b). \tag{A13}$$

The time dependence is made clearer by expanding the Gaussian term:

$$b(t) = \frac{\sigma_b(\sigma_u - \sigma_b)}{2\sigma_u\sqrt{\pi D}}t^{-3/2}\exp\left[-\frac{(\sigma_u - \sigma_b)^2}{4Dt}\right]. \tag{A14}$$

This probability density for binding is plotted in both panels of figure 5, where it is seen to be in excellent agreement with simulation data. It also yields some useful analytical results. At long times, the binding probability decreases with a dependence that is proportional to $t^{-3/2}$, which explains the scaling of the simulation data both for the time shortly before $\tau_{\text{n.g.}}$ and the time after $\tau_{\text{ter.}}$. Differentiating equation (A14) with respect to time shows that the most probable time for binding is at

$$\tau_{\text{gem.}} = \frac{(\sigma_u - \sigma_b)^2}{6D}. \tag{A15}$$

This equation is used to define $\tau_{\text{gem.}}$. For the binding of a ligand to the nearest neighbor receptor, the most probable time for binding can again be found from equation (A15), but now the initial separation is the receptor spacing. This yields the $\tau_{\text{n.g.}}$ definition given in the main text. A final property of equation (A14) is that the integral of $b(t)$ over all time yields the total probability that a ligand is absorbed by the sphere rather than diffusing away permanently; the result is $\phi = \sigma_b/\sigma_u$, as stated in equation (3).

## Glossary

*Binding radius.* The separation at which a pair of reactant molecules react with each other.

*Brownian dynamics.* A simulation method for molecular diffusion in which each molecule takes a step chosen from a Gaussian distribution, at each time step.

*Brownian motion.* Diffusive motion of a molecule that has been idealized to obey Fick's laws at all size and time scales, leading to an infinitely detailed trajectory.

*Diffusion limited.* Chemical reactions in which reactant diffusion is so slow that it completely determines the reaction rate.

*Geminate recombination.* The reaction between a pair of product molecules that arose from the same reactant molecule, back to yield a reactant. Here, it is the binding of a ligand to the same receptor from which it just dissociated.

*Ligand rebinding.* Synonymous with serial ligation.

*Probability density.* A distribution of a probability over space or time. The probability that a random variable falls within a small interval is the product of the probability density for that region and the width of the interval.

*Serial ligation.* A phenomenon in which a ligand sequentially binds and unbinds to many different receptors.

*Unbinding radius.* The initial separation between the products of a reversible reaction. It is also the physical distance between reactants outside of which interactions are negligible.

*Zero-crossing.* A point where a random walk crosses the plane at $z = 0$.

## References


[1] Sourjik V 2004 *Trends Microbiol.* **12** 569
[2] Noyes R M 1955 *J. Am. Chem. Soc.* **77** 2042
[3] McAdams H H and Arkin A 1997 *Proc. Natl Acad. Sci. USA* **94** 814
[4] Barkai N and Leibler S 2000 *Nature* **403** 267
[5] Arkin A, Ross J and McAdams H H 1998 *Genetics* **149** 1633
[6] Gillespie D T 1977 *J. Phys. Chem.* **81** 2340
[7] Meng T C, Somani S and Dhar P 2004 *In Silico Biol.* **4** 24
[8] Agmon N and Edelstein A 1995 *Biophys. J.* **68** 815
[9] Gopalakrishnan M *et al* 2005 *Eur. Biophys. J.* at press (doi:10.1007/s00249-005-0471-2)
[10] Lagerholm B C and Thompson N L 1998 *Biophys. J.* **74** 1215
[11] Lieto A M, Lagerholm B C and Thompson N L 2003 *Langmuir* **19** 1782
[12] Thompson N L, Burghardt T P and Axelrod D 1981 *Biophys. J.* **33** 435
[13] Kim H and Shin K J 1999 *Phys. Rev. Lett.* **82** 1578
[14] Popov A V and Agmon N 2001 *J. Chem. Phys.* **115** 8921
[15] Berg H C and Purcell E M 1977 *Biophys. J.* **20** 193
[16] Northrup S H 1988 *J. Phys. Chem.* **92** 5847
[17] Shoup D and Szabo A 1982 *Biophys. J.* **40** 33
[18] Valitutti S, Müller S, Cella M, Padovan E and Lanzavecchia A 1995 *Nature* **375** 148
[19] Wofsy C, Coombs D and Goldstein B 2001 *Biophys. J.* **80** 606
[20] Agmon N and Edelstein A L 1997 *Biophys. J.* **72** 1582
[21] Edelstein A L and Agmon N 1997 *J. Comput. Phys.* **132** 260
[22] Bren A and Eisenbach M 2000 *J. Bacteriol.* **182** 6865
[23] Maddock J R and Shapiro L 1993 *Science* **259** 1717
[24] Ames P, Studdert C A, Reiser R H and Parkinson J S 2002 *Proc. Natl Acad. Sci. USA* **99** 7060
[25] Bourret R B and Stock A M 2002 *J. Biol. Chem.* **277** 9625
[26] Kim S-H, Wang W and Kim K K 2002 *Proc. Natl Acad. Sci. USA* **99** 11611
[27] Shimizu T S *et al* 2000 *Nature Cell Biol.* **2** 792
[28] Alberts B *et al* 1994 *Molecular Biology of the Cell* 3rd edn (New York: Garland)
[29] Andrews S S and Bray D 2004 *Phys. Biol.* **1** 137
[30] Keizer J 1987 *Statistical Thermodynamics of Nonequilibrium Processes* (New York: Springer)
[31] Danielson M A, Biemann H-P, Koshland D E and Falke J J 1994 *Biochemistry* **33** 6100
[32] Dunten P and Koshland D E J 1991 *J. Biol. Chem.* **266** 1491
[33] Atkins P W 1986 *Physical Chemistry* 3rd edn (New York: W H Freeman and Co.)
[34] Hynes J T 1985 The theory of reactions in solution *Theory of Chemical Reaction Dynamics* ed M Baer (Boca Raton, FL: CRC Press)
[35] Agmon N 1984 *J. Chem. Phys.* **81** 2811
[36] Collins F C and Kimball G E 1949 *J. Colloid Sci.* **4** 425
[37] Rice S A 1985 Diffusion limited reactions *Comprehensive Chemical Kinetics* vol 25 ed C H Bamford, C F H Tipper and R G Compton (Amsterdam: Elsevier)
[38] Northrup S H, Allison S A and McCammon J A 1984 *J. Chem. Phys.* **80** 1517
[39] Berg H C 1993 *Random Walks in Biology* 2nd edn (Princeton, NJ: Princeton University Press)
[40] Edelstein A L and Agmon N 1993 *J. Chem. Phys.* **99** 5396
[41] Press W H, Flannery B P, Teukolsky S A and Vetterling W T 1988 *Numerical Recipies in C. The Art of Scientific Computing* (Cambridge: Cambridge University Press)
[42] The source code can be downloaded from the world wide web site: sahara.lbl.gov/∼sandrews/software.html.
[43] Crank J 1975 *The Mathematics of Diffusion* 2nd edn (Oxford: Oxford University. Press)
[44] Jackson J D 1998 *Classical Electrodynamics* 3rd edn (New York: Wiley)
[45] Mandelbrot B B 1983 *The Fractal Geometry of Nature* (New York: W H Freeman and Co.)
[46] Bornhorst J A and Falke J J 2001 *J. Gen. Physiol.* **118** 693
[47] Lagerholm B C and Thompson N L 2000 *J. Phys. Chem.* B **104** 863
[48] Levin M D, Shimizu T S and Bray D 2002 *Biophys. J.* **82** 1809
[49] Camacho C J, Kimura S R, DeLisi C and Vajda S 2000 *Biophys. J.* **78** 1094
[50] Northrup S H and Erickson H P 1992 *Proc. Natl Acad. Sci. USA* **89** 3338
[51] Elowitz M B, Surette M G, Wolf P-E, Stock J B and Leibler S 1999 *J. Bacteriol.* **181** 197
[52] Yi X and Weis R M 2002 *Biochim. Biophys. Acta* **1596** 28
[53] Shea L D, Neubig R R and Linderman J J 2000 *Life Sci.* **68** 647
[54] Stickle D and Barber R 1991 *Mol. Pharmacol.* **40** 276
[55] Duke T A J, LeNovère N and Bray D 2001 *J. Mol. Biol.* **308** 541
[56] Hedblom M L and Adler J 1983 *J. Bacteriol.* **155** 1463
[57] Bray D and Duke T 2004 *Ann. Rev. Biophys. Biomol. Struct.* **33** 53
[58] Carslaw H S and Jaeger J C 1959 *Conduction of Heat in Solids* 2nd edn (Oxford: Clarendon)